Merging of coherent structures in a separation bubble

J. W. Kurelek and S. Yarusevych[†]

Department of Mechanical and Mechatronics Engineering
University of Waterloo
200 University Ave. W., Waterloo, ON, Canada, N2L 3G1
[†]syarus@uwaterloo.ca

ABSTRACT

This work examines the spatio-temporal evolution and interaction of coherent structures in a laminar separation bubble (LSB) when left to develop naturally and excited acoustically. The investigation is carried out in a wind tunnel using a NACA 0018 airfoil model at a chord Reynolds number of 125 000 and an angle of attack of 4°. Excitation is provided by an external acoustic source and planar, time-resolved Particle Image Velocimetry is used to characterize both the streamwise and spanwise flow development. It is shown that the separation bubble is receptive to acoustic disturbances applied at the first subharmonic of the most unstable disturbance frequency in the natural LSB, leading to the inception, growth, and decay of velocity fluctuations in the separated shear layer. These velocity disturbances are shown to manifest through periodic vortex merging – a process that otherwise occurs randomly in the natural flow. Assessment of the spanwise flow topology reveals that structures merge in a non-uniform manner along the span, with localized merging occurring away from where streamwise-oriented bulges develop in the two vortices involved in the pairing process.

INTRODUCTION

For airfoils operating in the low Reynolds number regime ($Re_c = U_0 c/\nu \lesssim 10^6$), the suction side boundary layer is prone to separation, leading to stall or the formation of a laminar separation bubble, both of which adversely affect performance (Gaster, 1967; Carmichael, 1981). Due to a recent resurgence of applications where LSBs form on lifting surfaces, such as small-to-medium scale wind turbines and unmanned aerial vehicles (Fosas de Pando *et al.*, 2014; Mueller & DeLaurier, 2003), recent research efforts have been focused on the laminar-to-turbulent transition process within the separation bubble so that, ultimately, the process may be controlled and the performance losses mitigated.

Numerous investigations have examined separation bubble transition for flows over flat plates subjected to an adverse pressure gradient (e.g., Watmuff, 1999; Marxen *et al.*, 2013) and airfoils (e.g., Burgmann & Schröder, 2008; Jones *et al.*, 2010; Boutilier & Yarusevych, 2012). In either case, the initial stage of transition is characterized by the amplification of small-amplitude disturbances within a band of frequencies, shown to be primarily due to an inviscid Kelvin-Helmholtz type instability (Watmuff, 1999; Boutilier & Yarusevych, 2012). The later stages of transition are characterized by the continued growth of disturbances, leading to their non-linear interaction, the roll-up of the separated shear layer and the periodic shedding of vortices in the aft portion of the bubble (e.g., Burgmann & Schröder, 2008; Jones *et al.*, 2010; Marxen *et al.*, 2013).

Flow control studies employing a variety of actuators, including external acoustic excitation (Yarusevych *et al.*, 2006), synthetic jets (Greenblatt & Wygnanski, 2000) and plasma actuators (Rizzetta & Visbal, 2011; Yarusevych & Kotsonis, 2017), have shown that periodic excitation is capable of modifying the LSB and improving aerodynamic performance, with the effectiveness of the control strongly dependent on the amplitude and frequency of the excitation. Using controlled acoustic disturbances, Yarusevych *et al.* (2006) established a link between the most effective excitation frequency and that of the most amplified disturbances in the unperturbed flow, i.e., the fundamental frequency. The results have been corroborated by other investigators (Marxen *et al.*, 2015; Yarusevych & Kotsonis, 2017), who have gone on to show that such actuation accelerates transition in the separation bubble, thereby modifying the mean bubble topology, which in turn influences the stability characteristics.

The effects of forcing at subharmonics of the shear layer's fundamental frequency has gone largely unexamined in separation bubbles, despite having been shown to have significant effects on flow development in free shear layers (Ho & Huerre, 1984). Specifically, vortex merging occurs in naturally developing free shear layers (e.g., Miksad, 1972; Winant & Browand, 1974), and this process can be manipulated via subharmonic forcing (Ho & Huang, 1982). After disturbance growth at the fundamental frequency saturates, a subharmonic resonance mechanism gives rise to subharmonic disturbance growth (Kelly, 1967; Monkewitz, 1982). Thus forcing applied at the first subharmonic frequency accelerates growth of this mode, promoting vortex pairing and increasing the rate of momentum transfer across the layer (Ho & Huang, 1982).

Vortex merging has been observed to occur sporadically in separation bubbles (Lambert & Yarusevych, 2015; Kurelek *et al.*, 2016), however, the process has not been investigated in detail and its role in LSB development remains unclear. As such, the present investigation aims to analyze the spatio-temporal evolution and merging characteristics of coherent structures in natural and subharmonically forced LSBs via time-resolved Particle Image Velocimetry (PIV).

EXPERIMENTAL SETUP

Experiments were conducted in a recirculating wind tunnel at the University of Waterloo. The tunnel test section is 2.44 m long, 0.61×0.61 m in cross-section, and has a free-stream turbulence intensity of less than 0.1%. All experiments were conducted using a NACA 0018 airfoil model with a chord length, c, of 0.2 m and span of 0.61 m. An angle of attack, α, of 4° was investigated at a free-stream velocity of $U_0 = 9.6\,\mathrm{m\,s^{-1}}$ ($Re_c = 125\,000$). The flow was forced by means of acoustic excitation, with a subwoofer placed in the test section six chord lengths downstream of the airfoil. A 4189 Brüel and Kjær condenser microphone was used to characterize the sound pressure level (SPL) due to background noise and acoustic excitation at the airfoil surface. The excitation was supplied at the subharmonic of the natural flow's fundamental frequency. The subharmonic and fundamental frequencies are denoted by $\frac{1}{2}St_0$ and St_0, respectively, where the Strouhal number is defined as $St = fc/U_0$. The measured SPL for the natural and excitation cases are 87.1 and 89.5 dB, respectively.

Time-resolved, planar PIV was employed in the two configurations shown in Fig. 1, where the surface attached coordinate system is indicated. Here, the x, y, and z coordinates correspond to

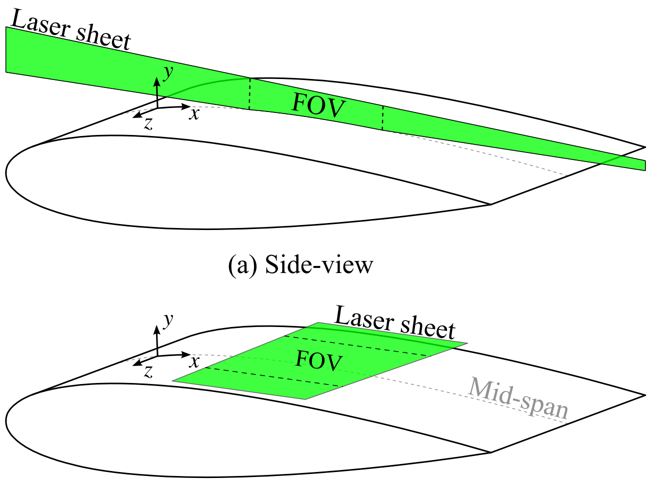

(a) Side-view

(b) Top-view

Figure 1. Experimental configurations for PIV measurements showing surface-attached coordinate system, whose origin is located at the leading edge and mid-span point.

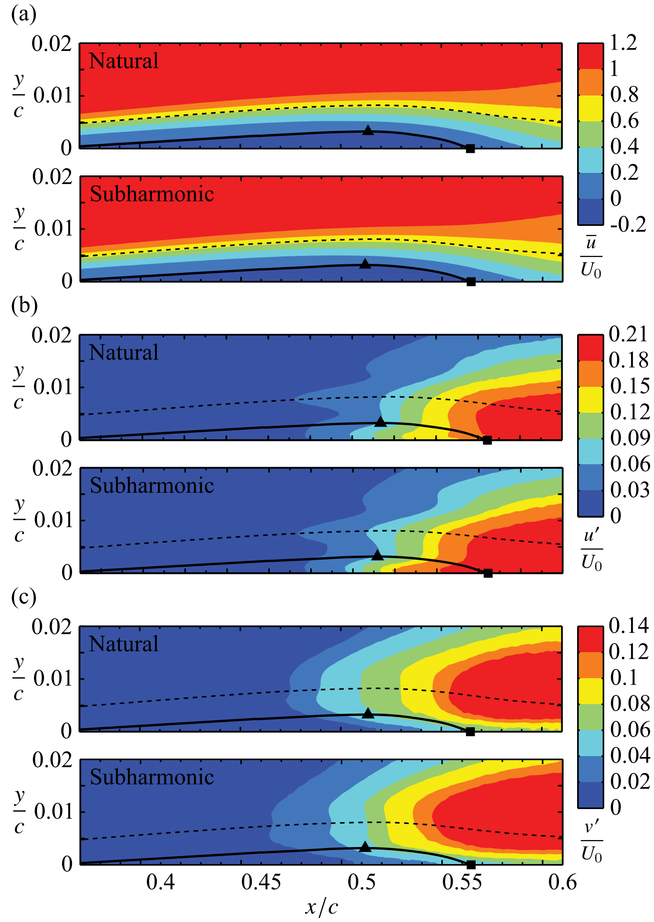

Figure 2. (a) Mean streamwise, $\overline{u}$, (b) streamwise rms, u', and (c) wall-normal rms, v', velocity contours. Solid lines mark the dividing streamlines. ▲ and ■ denote mean maximum bubble height and reattachment points, respectively. Dashed line indicates displacement thickness, δ^*.

the streamwise, wall-normal, and spanwise directions, respectively. The flow was seeded with a glycol-water based fog and illuminated by a Photonics DM20-527 Nd:YLF pulsed laser, whose beam was conditioned into a sheet approximately 1 mm in thickness. Particle images were acquired by two Photron SA4 high-speed cameras.

For the side-view PIV configuration (Fig. 1a), the laser sheet was positioned in the x-y plane and the cameras were fitted with 200 mm focal length lenses set to an aperture number of $f/4$. The fields of view were overlapped by 10%, covering a total area of 54×12.5 mm, and double-frame images were acquired at 3.8 kHz. For the top-viw configuration (Fig. 1b), the laser sheet was oriented parallel to airfoil surface within the investigated field of view (FOV), and the cameras were fitted with 105 mm focal length lenses set to $f/2.8$. The streamwise extent of the top-view FOV matched that of the combined side-view FOV, with the second camera employed to extend the FOV in the spanwise direction. Employing a 10% overlap, the total top-view FOV is 54×102 mm, with double-frame images acquired at 1.9 kHz.

Image sampling and processing were performed in LaVision's DaVis 8 software. For both configurations, an iterative, multi-grid cross-correlation scheme was used with an initial window size of 48×48 pixels and a final size of 16×16 pixels with 75% overlap. The resultant vector pitches in the PIV data are 0.12 and 0.24 mm for the side and top-view configurations, respectively. The random errors in the PIV measurements were evaluated using the particle image disparity method (Sciacchitano *et al.*, 2013, 2015), with the associated average uncertainties in the velocity fields estimated to be less than 6% and 6.5% for the side and top-view configurations, respectively.

RESULTS

The results presented here pertain to a separation bubble formed on the suction-side of a NACA 0018 airfoil at $Re_c = 125\,000$ and $\alpha = 4°$. In addition to leaving the flow to develop naturally, tonal acoustic excitation is applied at the first subharmonic frequency, $\frac{1}{2}St_0$, of the most unstable disturbance frequency in the natural LSB, measured to be $St_0 = 15.6$ ($f_0 = 750$ Hz).

Figure 2 presents time-averaged streamwise velocity, $\overline{u}$, and the root-mean-square (rms) of streamwise, u', and wall-normal, v', velocity fluctuations for the two cases investigated. The mean dividing streamline is determined for each case, whose intersection points with the surface are used to estimate the mean separation and reattachment points. The latter is indicated by the square markers in Fig. 2a, while the former lies just upstream of the measurement domain. The maximum bubble height location is also indicated and is found where the maximum wall-normal distance between the surface and dividing streamline occurs. Fig. 2a shows that the subharmonic excitation does not appreciably alter the mean topology of the bubble, with all changes in mean separation, maximum height, reattachment and displacement thickness falling within the experimental uncertainty of the measurement. Similarly, Figs. 2b–c indicates that the excitation does not alter the streamwise development of rms velocity significantly, most notably for the streamwise component (Fig. 2b). However, difference are detected in v' (Fig. 2c), as earlier disturbance amplification occurs when excited subharmonically, thus providing an preliminary indication that flow development is affected by the excitation.

The flow development within the unforced LSB is depicted in Fig. 3a using a sequence of instantaneous spanwise vorticity, ω, contours. Contours of the λ_2-criterion (Jeong & Hussain, 1995) are added to aid in the identification of coherent structures. The flow development is characterized by the periodic roll-up of the separated shear layer into vortices upstream of $x/c = 0.5$. These structures begin to deform within $0.5 < x/c < 0.55$, followed by the onset of breakdown to smaller scales at $x/c = 0.55$. Dashed lines are used to track the same structures between frames, with the

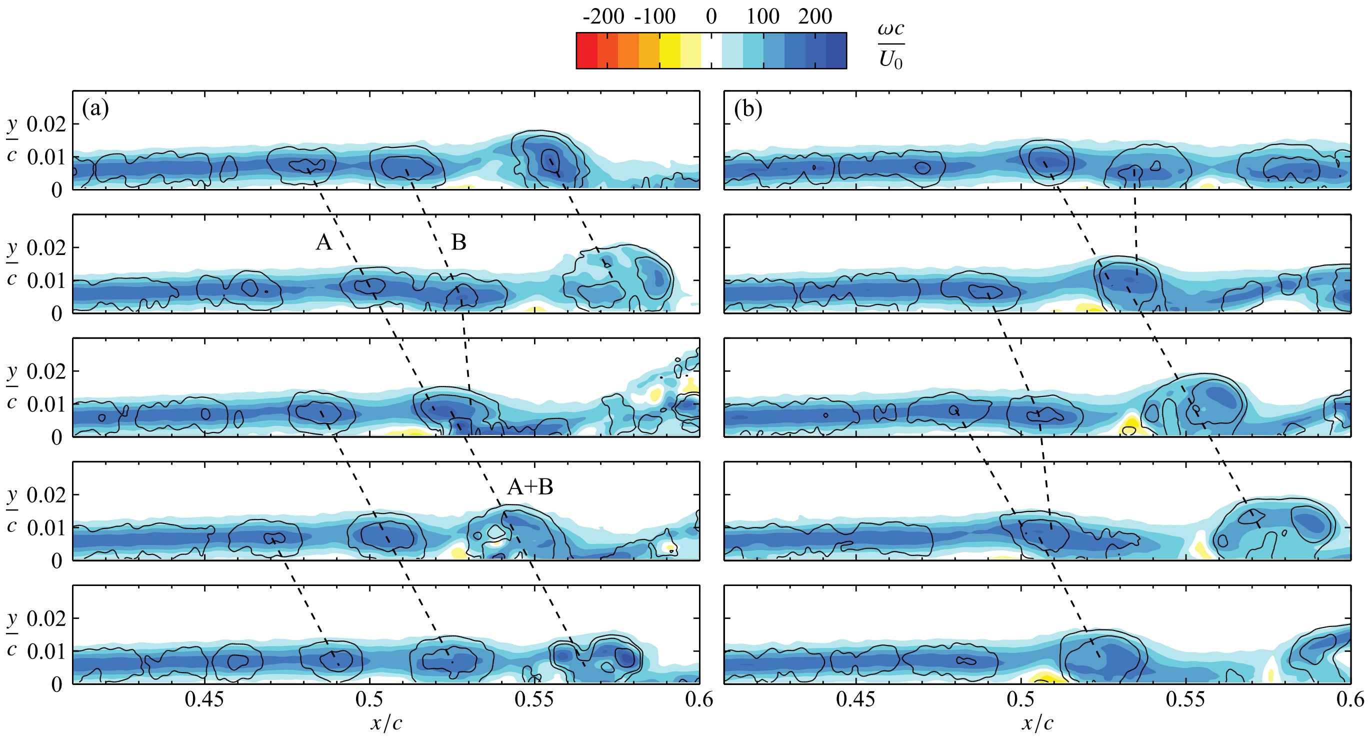

Figure 3. Instantaneous contours of spanwise vorticity, ω, for the (a) natural and (b) subharmonic excited flows. Consecutive frames are separated by $t^* = tU_0/c = 3.7 \times 10^{-2}$. Solid lines indicate λ_2-contours. Dashed lines trace the same vortices.

slope and streamwise spacing of the lines being representative of convective velocity and streamwise wavelength, respectively. The majority of structures shed in the naturally transitioning shear layer are characterized by similar convective velocities and wavelengths. However, sporadic merging of the shear layer vortices can occur, as captured for vortices A and B in Fig. 3a. It can be seen that the convective velocity of the downstream structure in the merging pair (B) decreases, while that of the upstream vortex remains nearly constant (A). Consequently, the distance between the vortex cores decreases and they merge, forming A+B. The observed process is in general agreement with the stages of vortex merging described by Cerretelli & Williamson (2003). The resulting merged vortex is separated from the nearest downstream vortex by approximately twice the average streamwise wavelength.

Figure 3b shows the LSB flow development for the case of subharmonic excitation, where, similar to the natural case (Fig. 3a), the separated shear layer rolls up into periodic vortices at $x/c \approx 0.5$, which then convect downstream, deform, and begin to break down to smaller scales. However, in contrast to the natural case, vortex merging is observed regularly throughout the entire recorded sequence for the subharmonic case. This is exemplified by the results in Fig. 3b, as all vortices initially identified in the roll-up region ($x/c > 0.53$) are involved in a pairing process.

To quantify and compare frequency content and streamwise growth of flow disturbances for the two cases, spectra of wall-normal velocity fluctuations along $y = \delta^*$ (dashed lines in Fig. 2) are computed and presented in Fig. 4. For the natural flow, Fig. 4a shows that disturbances within a band of frequencies centred on St_0 undergo convective amplification within $0.39 < x/c < 0.51$, with roll-up observed in the downstream part of this region in Fig. 3a. Beyond $x/c = 0.51$, the energy within the unstable frequency band is redistributed to a wider range of frequencies, consistent with the breakup of the rollers in the final stages of transition to turbulence. Spectra for the subharmonic excitation, Fig. 4b, show that the forcing at $\frac{1}{2}St_0$ does not alter the natural band of amplified disturbances

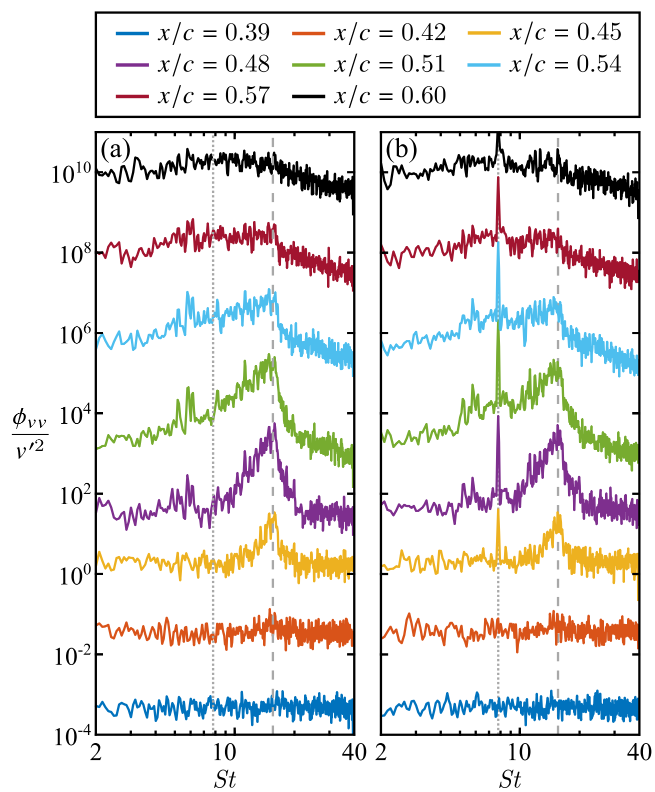

Figure 4. Frequency spectra of wall-normal velocity fluctuations, ϕ_{vv}, evaluated at $y = \delta^*$ for the (a) natural and (b) subharmonic excited flows. Spectra are normalized and incrementally stepped for clarity. Grey dashed and dotted lines denote St_0 and $\frac{1}{2}St_0$, respectively.

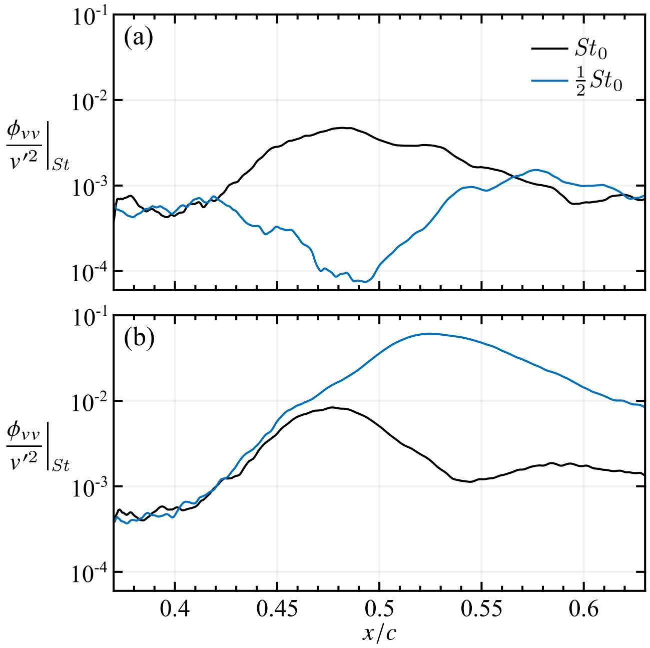

Figure 5. Streamwise growth of frequency filtered spectral energy within the separated shear layer for the (a) natural and (b) subharmonic excited flows.

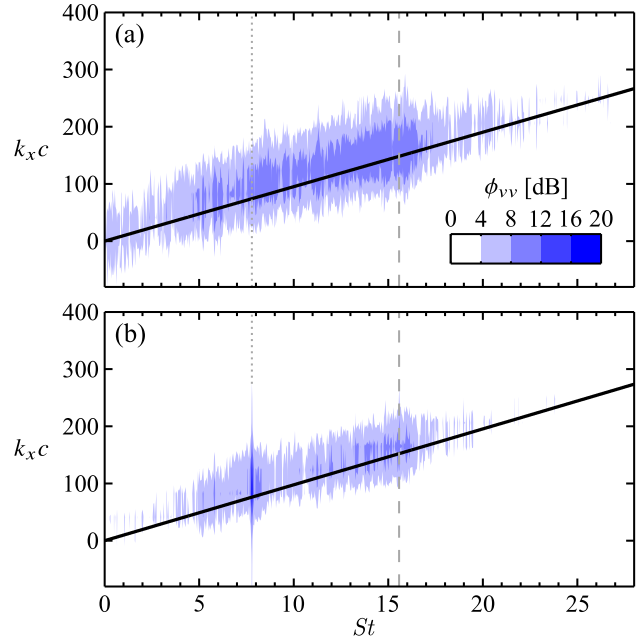

Figure 6. Wavenumber-frequency spectra of wall-normal velocity fluctuations in the separated shear layer for the (a) natural and (b) subharmonic excited flows. Solid black line is a linear fit estimating the convective ridge. Grey dashed and dotted lines denote St_0 and $\frac{1}{2}St_0$, respectively

appreciably, however, significant velocity fluctuations at $\frac{1}{2}St_0$ occur in the flow at and beyond $x/c = 0.45$. The associated spectral energy content is then amplified within $0.45 < x/c < 0.51$, which then decays further downstream. The observed strong frequency-centred activity at $\frac{1}{2}St_0$ is attributed to the periodic passage of disturbances characterized by twice the wavelength but of similar convective velocity to the main shear layer vortices, which is consistent with the characteristics of the merged vortices seen in Fig. 3b. Thus, supporting the analysis of the time-resolved flow development, these results imply that subharmonic forcing promotes periodic vortex merging in an LSB, similar to that observed in free shear layers (Ho & Huang, 1982). Furthermore, the absence of significant spectral peaks at $\frac{1}{2}St_0$ in Fig. 4a substantiates that merging occurs randomly in the unforced bubble.

Further parallels can be drawn between the present results and the vortex merging characteristics of free shear layers. Ho & Huang (1982) showed that periodic merging coincides with the growth of perturbation energy at the subharmonic frequency for acoustically forced free shear layers. A similar analysis is employed here, where the spectral energy components of shear layer disturbances associated with St_0 and $\frac{1}{2}St_0$ are computed and presented in Fig. 5. When left to develop naturally (Fig. 5a), disturbance amplification is detected at St_0 within $0.42 \leq x/c \leq 0.46$. The growth of disturbances leads to a saturation of the fundamental mode by $x/c \approx 0.48$, which falls within the roll-up region, followed by decay. The onset of the subharmonic amplification in this region is attributed to the redistribution of the spectral energy content to a broad frequency range during the later stages of the transition process (Fig. 4a). In contrast, in the case of subharmonic excitation (Fig. 5b), both the fundamental and subharmonic modes undergo initial amplification, with both modes having approximately equal growth rates. The fundamental mode then saturates at approximately the same streamwise locations as that of the natural case, while the subharmonic mode continues to grow, reaching its maximum energy content at approximately $x/c = 0.52$. The streamwise location where this maximum is reached coincides with where vortex merging is observed in Fig. 3b, thus supporting the assertions of Ho & Huang (1982). In fact, the trends present in Fig. 5b agree will with those reported by Ho and Huang (see their Figs. 15 and 16), which further reinforces the significance of the role the Kelvin-Helmholtz instability plays in the transition process of a separation bubble. However, two important distinctions between the present results and free shear layers must be highlighted. The secondary harmonic resonance mechanism, which has been proposed for free shear layers (Kelly, 1967; Monkewitz, 1982), dictates that the growth of the subharmonic mode must follow the saturation of the fundamental mode, in addition to occurring in both forced and natural free shear layers. In the present results, growth of the subharmonic mode does not occur in the natural case, and when excited, the growth of these two modes occurs concurrently. Such differences are attributed to the evident differences in the mean topology between free shear layers and LSBs, leading to changes in stability characteristics.

To further characterize the shed and merged coherent structures within the separation bubble, two-dimensional, wavenumber-frequency spectra are computed using wall-normal velocity sampled along $y = \delta^*$. The spectra are computed in time and along x, with the resulting streamwise wavenumber denoted by k_x. For the natural case (Fig. 6a), spectral energy is concentrated along a line of nearly constant slope, which is commonly referred to as the convective ridge (e.g., Howe, 1998). Along the convective ridge, the disturbance wavenumber and frequency are related by their convective velocity, $U_c = 2\pi f/k_x$. From Fig. 6a, the wavenumber and convective velocity corresponding to St_0 are $k_x c = 150$ and $U_c/U_e = 0.55$, respectively, where U_e is the separation bubble edge velocity and is taken to be $1.2U_0$ (Fig. 2a). The determined convective velocity falls within the range of values, $0.3 \lesssim U_c/U_e \lesssim 0.6$, observed in previous investigations (Burgmann & Schröder, 2008; Boutilier & Yarusevych, 2012).

Figure 6b shows that subharmonic acoustic excitation leads to high concentration of spectral energy towards the excitation frequency, $\frac{1}{2}St_0$. The convective ridge is once again identified, with a disturbance convective velocity of $U_c/U_e = 0.54$ closely match-

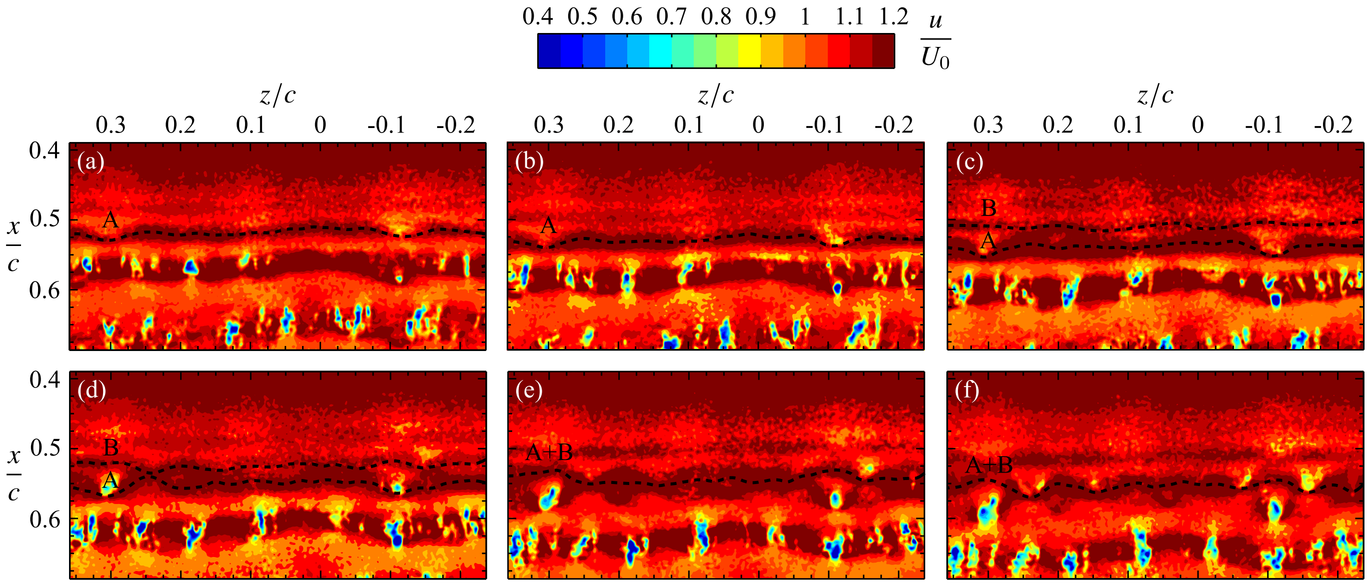

Figure 7. Instantaneous streamwise velocity for the subharmonic excited flow. Flow is from top to bottom. Consecutive frames are separated by $t^* = 2.5 \times 10^{-2}$. Dashed lines indicate smoothed spline fits to the centre of selected structures.

ing that of the natural case. Therefore, consistent with the convective velocities ascertained from the vortex traces in Fig. 3, the occurrence of period vortex merging does not alter the convective velocity of the disturbances significantly. Furthermore, along the convective ridge in Fig. 6b, the wavenumber corresponding to the most amplified frequency is $k_x c = 76$. This confirms that subharmonic excitation promotes disturbance amplification at half the natural frequency and wavenumber, inducing regular merging of the shear layer vortices, as seen in Fig. 3b.

PIV measurements from the top-view configuration (Fig. 1b) allow for the analysis of both streamwise and spanwise aspects of the vortex merging process. The measurement plane was positioned such that it passed through the top-halves of the roll-up structures, thus allowing for their identification as periodic spanwise bands of high streamwise velocity in the planar images. Such bands are revealed in the streamwise velocity contours of Fig. 7, which depicts the flow development for the case of subharmonic excitation. Coherent and spanwise uniform structures are first identifiable at $x/c \approx 0.5$, which is consistent with where roll-up is observed in Fig. 3b. At and beyond formation, significant spanwise undulations develop in the vortex filaments, which intensify as the structures convect downstream. This leads to the onset of the breakup to smaller scales seen for $x/c > 0.6$.

The merging process between two shear layer vortices, identified as A and B, is captured in Fig. 7. In Fig. 7a, vortex A convects downstream while developing spanwise undulations which are most notable at $z/c = -0.1$ and 0.3 in Figs. 7a–c, where the vortex filament bulges forward in the streamwise direction. Concurrently, vortex B rolls up and also develops spanwise undulations in Figs. 7c–d. The merging process between A and B begins to take place in Fig. 7d, as the vortex filaments intertwine within $-0.05 \lesssim z/c \lesssim 0.25$, while the structures do not merge at the spanwise locations where the forward streamwise bulges developed in A. The merged structure, labelled as A+B, then continues to convect downstream through Figs. 7e–f, while retaining two separate vortex filaments within some spanwise segments, e.g. at $z/c \approx -0.1$ and 0.3. Thus, the results suggest that vortex merging in a separation bubble does not occur uniformly along the span, with the spanwise undulations that develop in the vortex filaments playing an intrinsic role.

CONCLUSIONS

Flow development and the merging characteristics of shear layer vortices were investigated experimentally within a separation bubble formed on a NACA 0018 airfoil at a chord Reynolds number of 125 000 and an angle of attack of 4°. The flow field was assessed via wind tunnel tests carried out using time-resolved, planar, two-component PIV. The measurements were performed in two different configurations, allowing for the analysis of both the streamwise and spanwise flow development. Owing to the pervasiveness of vortex merging in free shear layers forced acoustically at a subharmonic frequency, the technique was employed here to examine if similar effects manifest in separation bubbles.

For the investigated conditions, a suction-side separation bubble formed when the flow was left to develop naturally, the mean topological features of which did not change appreciably in the presence of the relatively low amplitude acoustic subharmonic excitation. However, the separated shear layer dynamics were found to be receptive to these acoustic disturbances, which led to the inception, growth, and decay of velocity fluctuations at the subharmonic frequency, similar to that observed in free shear layers (Ho & Huang, 1982; Ho & Huerre, 1984). Furthering the comparison with free shear layers, growth of the subharmonic velocity disturbances saturated at a streamwise location coinciding with where vortex merging was predominantly observed to occur. However, notable differences distinctions with free shear layers were found; namely the growth of the subharmonic and fundamental modes occurred concurrently in the LSB, while the subharmonic mode did not amplify in the natural flow conditions.

The subharmonic velocity disturbances observed in the excited flow were shown to manifest through the periodic merging of the separated shear layer roll-up vortices, while merging occurred randomly in the natural flow. The shear layer vortices were characterized using spectral analysis, showing that their predominant wavenumber reduced to half of that in the natural flow, while their convective velocity remained essentially unchanged. Assessment of the spanwise behaviour of the vortex merging process revealed that structures merge in a spanwise non-uniform manner, with localized merging occurring away from where forward streamwise-oriented bulges develop in the downstream vortex of the merging pair.

ACKNOWLEDGEMENTS

The authors gratefully acknowledge the Natural Sciences and Engineering Research Council of Canada for funding this work.

REFERENCES

Boutilier, M. S. H. & Yarusevych, S. 2012 Separated shear layer transition over an airfoil at a low Reynolds number. *Phys. Fluids* **24** (8), 084105.

Burgmann, S. & Schröder, W. 2008 Investigation of the vortex induced unsteadiness of a separation bubble via time-resolved and scanning PIV measurements. *Exp. Fluids* **45** (4), 675–691.

Carmichael, B. H. 1981 Low Reynolds Number Airfoil Survey. *Tech. Rep.*. NASA Contract Report No. 165803.

Cerretelli, C. & Williamson, C. 2003 The physical mechanism for vortex merging. *J. Fluid Mech.* **475**, 41–77.

Fosas de Pando, M., Schmid, P. J. & Sipp, D. 2014 A global analysis of tonal noise in flows around aerofoils. *J. Fluid Mech.* **754**, 5–38.

Gaster, M. 1967 The Structure and Behaviour of Laminar Separation Bubbles. *Aeronaut. Res. Counc.* **RM 3595**.

Greenblatt, D. & Wygnanski, I. J. 2000 The control of flow separation by periodic excitation. *Prog. Aerosp. Sci.* **36** (7), 487–545.

Ho, C.-M. & Huang, L.-S. 1982 Subharmonics and vortex merging in mixing layers. *J. Fluid Mech.* **119**, 443–473.

Ho, C.-M. & Huerre, P. 1984 Perturbed Free Shear Layers. *Annu. Rev. Fluid Mech.* **16** (1), 365–424.

Howe, M. S. 1998 *Acoustics of Fluid-Structure Interactions*. Cambridge University Press.

Jeong, J. & Hussain, F. 1995 On the identification of a vortex. *J. Fluid Mech.* **285**, 69–94.

Jones, L. E., Sandberg, R. D. & Sandham, N. D. 2010 Stability and Receptivity Characteristics of a Laminar Separation Bubble on an Aerofoil. *J. Fluid Mech.* **648**, 257–296.

Kelly, R. E. 1967 On the stability of an inviscid shear layer which is periodic in space and time. *J. Fluid Mech.* **27** (04), 657–689.

Kurelek, J. W., Lambert, A. R. & Yarusevych, S. 2016 Coherent Structures in the Transition Process of a Laminar Separation Bubble. *AIAA J.* **54** (8), 2295–2309.

Lambert, A. R. & Yarusevych, S. 2015 Analyzing Vortex Dynamics in the Laminar Separation Bubble via Surface Pressure Measurements. In *45th AIAA Fluid Dyn. Conf. Exhib.*. Dallas, TX, USA.

Marxen, O., Kotapati, R. B., Mittal, R. & Zaki, T. 2015 Stability analysis of separated flows subject to control by zero-net-mass-flux jet. *Phys. Fluids* **27** (2), 024107.

Marxen, O., Lang, M. & Rist, U. 2013 Vortex Formation and Vortex Breakup in a Laminar Separation Bubble. *J. Fluid Mech.* **728**, 58–90.

Miksad, R. W. 1972 Experiments on the nonlinear stages of free-shear-layer transition. *J. Fluid Mech.* **56** (04), 695.

Monkewitz, P. A. 1982 Influence of the velocity ratio on the spatial instability of mixing layers. *Phys. Fluids* **25** (7), 1137–1143.

Mueller, T. J. & DeLaurier, J. D. 2003 Aerodynamics of Small Vehicles. *Annu. Rev. Fluid Mech.* **35** (1), 89–111.

Rizzetta, D. P. & Visbal, M. R. 2011 Numerical Investigation of Plasma-Based Control for Low-Reynolds-Number Airfoil Flows. *AIAA J.* **49** (2), 411–425.

Sciacchitano, A., Neal, D. R., Smith, B. L., Warner, S.O., Vlachos, P. P., Wieneke, B. & Scarano, F. 2015 Collaborative framework for PIV uncertainty quantification: comparative assessment of methods. *Meas. Sci. Technol.* **26** (7), 074004.

Sciacchitano, A., Wieneke, B. & Scarano, F. 2013 PIV uncertainty quantification by image matching. *Meas. Sci. Technol.* **24** (4), 045302.

Watmuff, J. H. 1999 Evolution of a wave packet into vortex loops in a laminar separation bubble. *J. Fluid Mech.* **31**, 119–169.

Winant, C. D. & Browand, F. K. 1974 Vortex pairing: the mechanism of turbulent mixing-layer growth at moderate Reynolds number. *J. Fluid Mech.* **63** (02), 237–255.

Yarusevych, S., Kawall, J. G. & Sullivan, P. E. 2006 Airfoil Performance at Low Reynolds Numbers in the Presence of Periodic Disturbances. *J. Fluids Eng.* **128** (3), 587.

Yarusevych, S. & Kotsonis, M. 2017 Effect of Local DBD Plasma Actuation on Transition in a Laminar Separation Bubble. *Flow, Turbul. Combust.* **98** (1), 195–216.